Control of a Pneumatically Actuated Joint for Wearable Supernumerary Robotic Limbs Application

by

Roger Lo

Submitted to the Department of Mechanical Engineering in Partial Fulfillment of the Requirements for the Degree of

Bachelor of Science in Mechanical Engineering

at the

Massachusetts Institute of Technology

June 2016

Signature redacted

Signature of Author: _____
Department of Mechanical Engineering
May 6, 2016

Signature redacted

Certified by: _____
Harry Asada
Professor of Mechanical Engineering
Thesis Supervisor

Signature redacted

Accepted by: _____
Anette Hosoi
Professor of Mechanical Engineering
Undergraduate Officer

Control of a Pneumatically Actuated Joint for Wearable Supernumerary Robotic Limbs Application

by Roger Lo

Submitted to the Department of Mechanical Engineering in Partial Fulfillment of the Requirements for the Degree of

Bachelor of Science in Mechanical Engineering

June 2016

Abstract

Presented is work on the development of the Supernumerary Robotic Limbs project, headed by Federico Parietti in the d'Arbeloff Labs under Prof. Harry Asada. Specifically, this paper focuses on the integration of lightweight, pneumatic systems for prismatic joint actuation, and the various control schemes studied. This joint serves as the leg of the robot, and extends from the hip of the wearer to contact the ground. The design consists of a two-way pneumatic cylinder inside a load bearing carbon fiber sleeve, actuated with a nominally closed 5-3 way solenoid valve, and weighs in at <1kg per actuator. The positional control scheme is closed via tracking from a linear magnetopotentiometer, while the force control scheme utilizes both the positional tracking as well as a load cell at the foot of the leg. System modeling of the actuator dynamics allowed for development of a model based proportional control method. Optimization of the proportional gain and system delay time produced a rise time of 200ms given a step input command for a 250mm stroke. The developed scheme was implemented in the full wearable system to assist a human support weight in crouched positions and standing up from a sitting position. Initial testing has shown the effectiveness of the power, compactness and compliance of pneumatic systems in a wearable robotic device.

Thesis Supervisor: Harry Asada

Title: Professor of Mechanical Engineering

Table of Contents

1 Introduction

Wearable robotics provide a wide range of applications for human use and is a rapidly expanding area of study in the field of robotics. The integration of wearable robotics hopes to improve the lives of humans through rehabilitation, assistance and augmentation of our everyday capabilities. Many current wearable robots conform to the human geometry, such as exoskeletons, using the body as a reference to supplement existing behavior. [1] The Supernumerary Robotic Limbs (SRL) project aims to provide a means for an entirely new area of human functionality by adding limbs that are not constrained by pre-existing human movement. Supplementing the human body with this robot allows the concept of innovative augmentation to be researched, providing a new avenue for wearable robotic development.

The system is designed to be easily worn in a comfortable harness, with two robotic limbs extending from the user's hip. The legs are completely independent of the rest of the body and will therefore enable performance of tasks normally outside the user's capabilities. The target application for the SRL is locomotion assistance and rehabilitation. Traditional assistive systems resemble exoskeletons, follow the structure of the human leg and are extremely heavy and inefficient to use. The need to tightly pair the robotic joints to the legs can potentially obstruct or even hurt the user. [1] With the freedom of the SRL design, users are free from discomfort or obstruction by the robotic joints, while still being able to reap its assistive power.

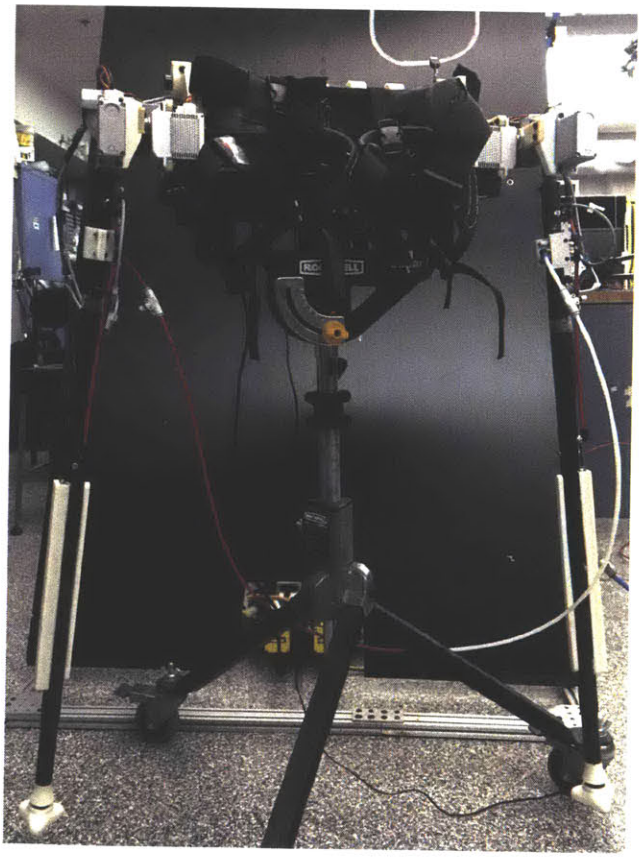

Fig. 1: Fully assembled prototype. The harness and base is sitting on a raised platform.

1.1 Design of Joints and Actuators

The driving mechanical design factors that will enable this to be a successful robot are weight and robustness. For comfortable use, the wearer must not be strained by the weight of the robot, which severely limits the choices for actuation methods. The robot must also provide reliable support for the entire human body, which calls for a structurally strong construction. The SRL prototype has been designed with these factors in mind.

1.1.1 Ball Joint/Actuation

At the location where the limb attaches to the hip exists a 2DOF ball joint mechanism, actuated with two powerful hobby grade servo motors [Hitec HS-1000SGT]. The choice of these specific servos was the result of an extensive study on commercially available hobby grade servo motors, comparing their torque to weight ratio and form factor for optimal performance and integration in this wearable system. [See Appendix A] This joint provides the angular control of the limb, much like a human shoulder would for the arm. The joint mechanism and mounts were manufactured via additive 3D printing, from technology developed by MarkForged, Cambridge, MA. The printers used allowed for rapid prototype and construction of lightweight yet durable custom nylon and carbon fiber composite parts, reducing material to only where it is absolutely necessary. The light, compact design of this joint rivals the mechanical stiffness of aluminum and is fully capable of supporting the loads required. [See Appendix A]

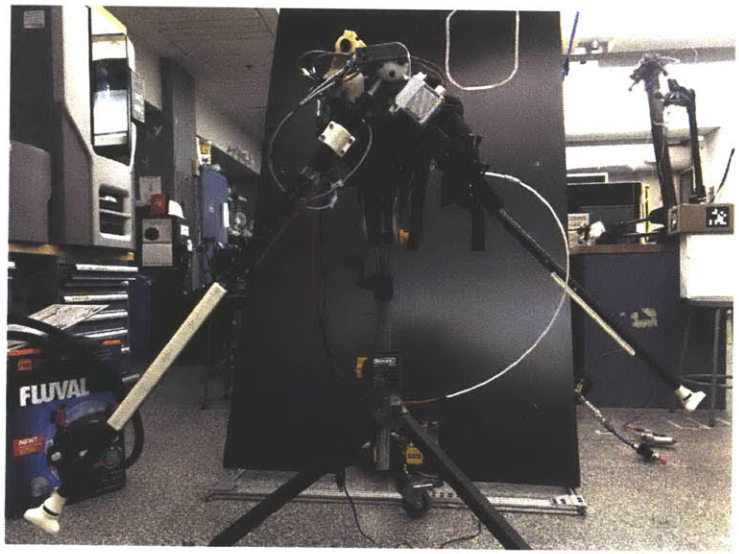

Fig. 2: (Left) Ball joints actuated at angles to showcase range of the workspace. (Right)

1.1.2 Linear Joint/Actuation

The leg itself consists of a 1DOF prismatic joint that serves to extend and retract the end point of the leg, providing control of contact with the ground and the force necessary to lift the weight of the wearer. As shown in Fig. 1, the leg consists of a pneumatic cylinder and piston, encased in carbon fiber tubes that act as a bearing structure against side loads to the piston, as well as extending the reach of the leg. Previous prototypes of this system utilized a Firgelli servo linear actuator, which relied on a heavy-duty gear motor and a long lead screw. While the control of this kind of system is easily implemented and well understood, its maximum travel velocity was

limited to 10mm/s and weighs in at close to 2kg. As a comparison, the entire pneumatic cylinder system weighs in at less than 1kg and demonstrates a max velocity of close to 1m/s, while providing the same static force capability.

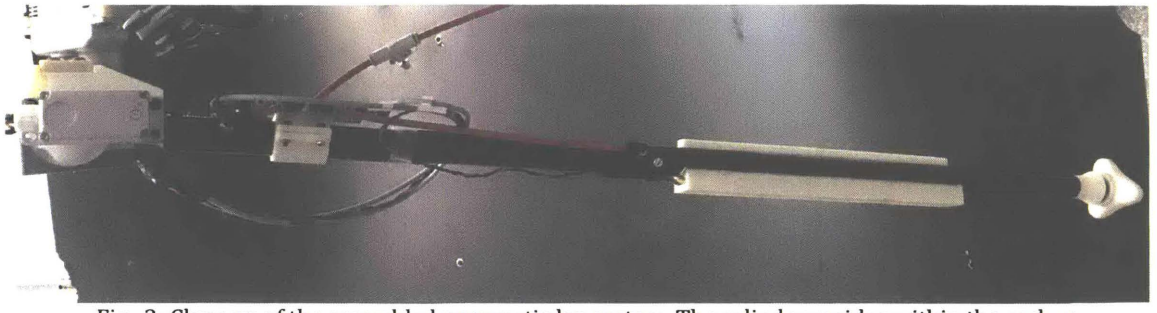

Fig. 3: Close up of the assembled pneumatic leg system. The cylinder resides within the carbon fiber tubing.

1.1.3 Sensors and Electronics

Commercially produced off-the-shelf position sensing cylinders generally do not provide the resolution of position sensing required by this project, typically only incorporating magnetic "trip" sensors that indicate when the piston has passed a location. To achieve closed loop sensing, a magnetic potentiometer is affixed to the upper half of the leg, while movement of the piston is coupled with the movement of a magnet on the electrical tracks of the sensor. This provides a simple, lightweight solution to position feedback that does not require incredible precision in manufacturing and assembly, as the coupling is not mechanical but induced by the magnet. A load cell is placed at the base of the robotic leg, and through use of an instrumentation amplifier chip is able to provide endpoint load feedback in the direction of actuation as well.

Control of the system is achieved through use of an Arduino MEGA. Implementation of actuation and control schemes have all been written directly onto the Arduino for fast loop cycling. Data regarding the sensors and timing are sent for logging through a serial communication with a computer.

1.2 General Remarks

From bench top testing, the behavior of this pneumatic system can be characterized and utilized to fuel design of control schemes that provide the desired behavior in the full system. The two schemes explored in this paper are a positional proportional control and a force control scheme, both stemming from an actuation method that is discontinuous and limited to a binary on/off signal to the input valves.

The simplicity of this design ensures that no extra components such as pressure regulators, pressure sensors, mechanical gears or linkages, or motors, will increase the weight of this wearable robot and render it useless in application. An adherence to keeping the weight low enough as to not cause fatigue or discomfort to the wearer limits the ability for the actuator to be controlled in more known robotic settings. Thus, intelligent control of the system will be required given the restraints the design has imposed on the actuation in order to achieve the robust functionality required.

2 Literature Review

To supplement the study of integrating these pneumatic cylinders into this robotic system, prior literature has been referenced, with the aims of supporting and facilitating the testing process. Comparisons between the SRL system and prior work will also be conducted to evaluate performance of the proposed schemes.

2.1 Historical and Modern Study

Pneumatic cylinders have long been an attractive method of actuation for high power, low weight systems. The abundance of the fluid medium, air, makes it very accessible to provide movement in most environments. The simplicity of the mechanical system, without the need for electrical or magnet rotors, internal combustion, or complex mechanical gears, make them reliable and easy to maintain. They have shown their usefulness in applications such as assembly line automation, construction (scissor lifts, excavators, jackhammers), and robotics (grippers, manipulators).

To that end, extensive research has been conducted to study these systems to improve behavior and control. As early as 1989, [2] developed control of a pneumatic cylinder system that could take 37kg loads up to 250mm strokes with ±1mm accuracy, within a second, showcasing the possibilities of using these systems without the need for mechanical stops. More complex, PID control algorithms were researched, such as [3] where a pneumatic system exhibited a 180ms rise time for a 64mm stroke. As improvements in computing power and accessibility increased, the capabilities to which pneumatic actuation could be controlled expanded. In 2005, [4] developed a modified PWM algorithm with on/off solenoid valves, along with a learning neural network algorithm on the position, velocity and acceleration control parameters that allowed for automated external load classification. As more research creates more intelligent control of these pneumatic systems, the area for which pneumatic cylinders can be applied grows vastly.

2.2 Modeling

Modeling the physics behind the actuation has also been critical to increasing development of these control schemes. At the core of the proposed design is the solenoid on/off valve, which allows the air from the pressure supply into the pneumatic chambers to provide the force required. The subtleties of this system arise in many non-linearities and unknowns, making it difficult to approach control without a learned approach. [5] investigated the physical relations between the electromagnetic, mechanical and fluid subsystems in these valves, experimentally validating their results to provide a useful simulation tool for pneumatic behavior. Their characterization method, using theory to predict system unknowns and measuring the unknowns to complete the system model, is similarly utilized in this paper. [6] developed a model of relating mass flow rates within pneumatic cylinders to pressure profiles within the chambers, allowing them to predict behavior a pneumatically actuated 44 DOF humanoid robot. Given the extensive prior research done on modeling these systems, a model based approach for control seems fairly attainable.

For the benefit of this project, many of the prior researchers' approaches have been utilized to develop the modeling and control schemes presented in this paper. Modeling equations and control schemes are implemented for use in this novel wearable setting to understand the benefits of these existing frameworks for wearable robotics. The application of the pneumatic system thus seems appropriate for study of this robotic system, and as discussed in later sections, possibly provides an innovative avenue for pneumatic cylinders in the realm of wearable robotics.

3 Technical Detail of Pneumatic System

To provide a complete basis for which the parameters for modeling have been founded upon, as well as the setup for all experimental data and testing, an exhaustive technical detail of the leg system follows.

3.1 Commercial Components

Many components of the leg system are off the shelf parts, chosen for their lightweight and compact nature. The cylinder is an aluminum 7/8" bore, 300mm stroke, two-way piston from Numatics. [See Appendix A] The two ports are connected via push-to-connect fittings onto 5mm pneumatic tubing, which provides airflow from the valve. The valve is a 5/2 way nominally closed solenoid valve from Festo. [See Appendix A] Because this valve has two output ports, only one solenoid is required per leg. The valve is connected to an inline flow regulator that acts as a safety check as well as setting the pressure of operation of the system. These are connected to the lab pressure line, which has an upper limit of 690,000Pa (100PSI). Future design of this prototype will attempt to pull away from a tethered approach, utilizing portable pressure supplies from either an air compressor or a compressed air tank similar to those used in paintballing.

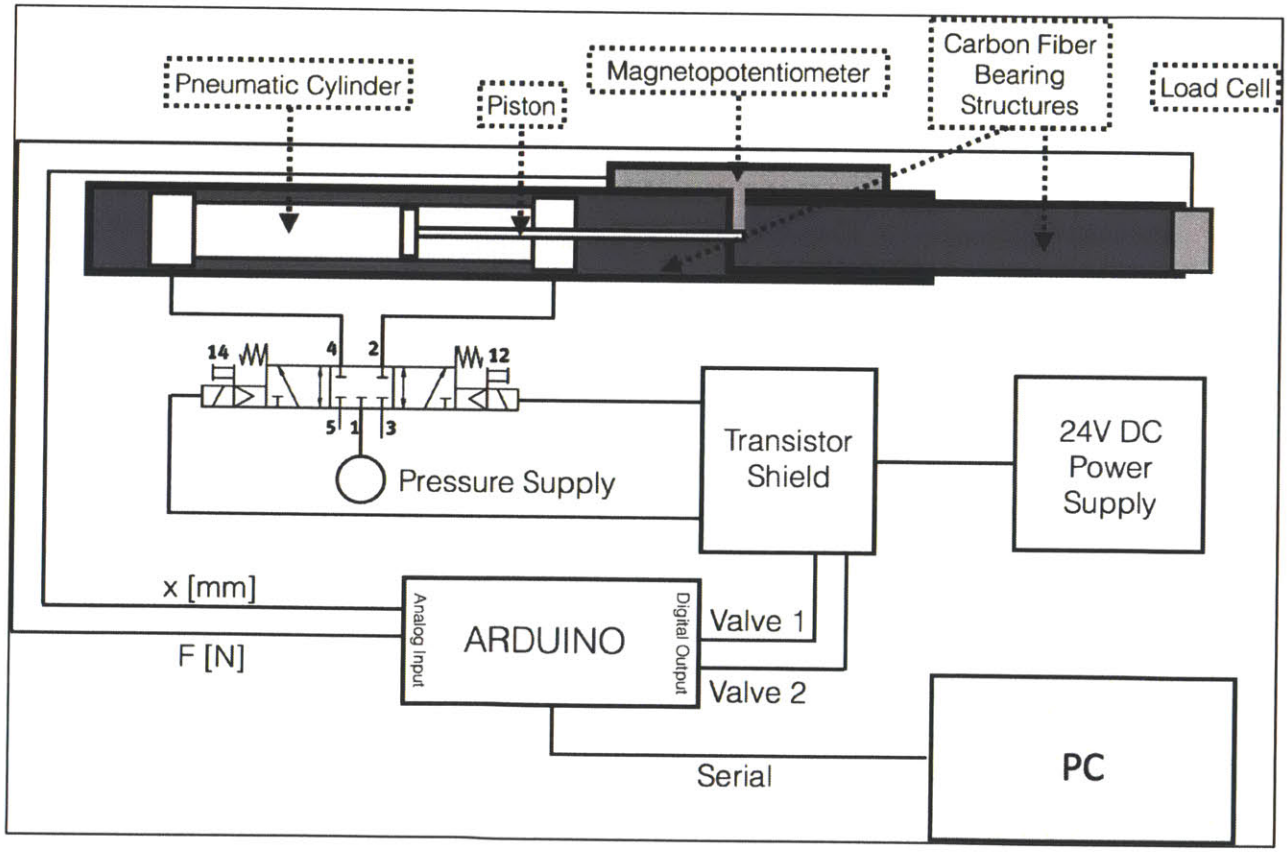

Fig. 4: Schematic of the leg system. There are two legs in the system, but only one Arduino is necessary for processing.

3.2 Custom Components

Custom components of this system have been designed to be lightweight and compact, with a form factor similar to that of a cane so as not to seem unnatural for human use. A custom 3D-printed carbon fiber composite strut extends from the ball joint system to connect to the length of the leg. This is secured to the upper carbon fiber tube that encases the body of the cylinder. The piston is connected to a second tube that fits snugly within the inner diameter of the upper tube, providing a low friction, compact bearing system against side loads to the thing piston rod. Custom aluminum mounts connect the cylinder and piston to the carbon fiber tubes. The upper tube has waterjetted slots that provide access for a link between the piston and the magnetopotentiometer. This link consists of a socket head cap screw extending from the inner tube with two small neodymium magnets embedded in the cap, positioned to be directly underneath the rails of the potentiometer. The sensor is attached to a 3D printed plastic fixture that rigidly attaches to the tube in line with the waterjetted slots. A second screw rides within the slot on the other side of the tube, preventing the piston from rotating along its axis. The foot of the leg is designed to have a three-point rubber contact, providing stable slip-free support from the ground. It is loosely linked to the base of the leg via a rubber connector, which allows for the plane of the foot to bend relative to the axis of the leg. Beneath this contact sits the load cell. See fig. 5 for a CAD model of this system and picture.

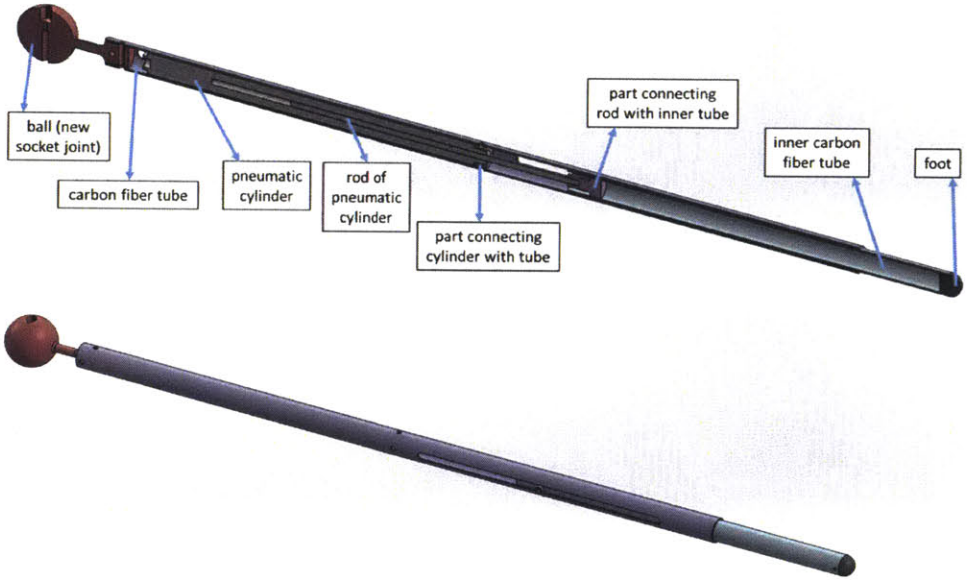

Fig. 5: (Top) Cross-Section of the prismatic joint system. (Bottom) CAD model of the prismatic joint system, without the sensors or valves.

4 Theoretical Modeling

Pneumatic systems exhibit large latency times that can be hazardous for simple control systems. Due to the compressibility of the medium, there is a significant delay between command signals and actuation, on the order of 100 milliseconds. [6] The non-linearity of the system makes it difficult to control without system modeling and characterization; early attempts resulted in jittery motion and non-converging behavior. In order to develop a robust control system, it is necessary to understand the physical behavior of the system and utilize this to fuel a model based control scheme.

4.1 Position Profile

For this study, the pneumatic and mechanical aspects of the system are modeled. The electromagnetic aspect, namely the control signal into the solenoid valve, is assumed to have a much smaller latency time than the rest of the system and is equated to be an instantaneous step input. From part specifications given by Festo, the solenoid valve exhibits a 10ms valve opening time, and a 30ms closing time. The area of the orifice where the valve allows air to flow is assumed to be linear [6] with time during these periods of solenoid movement, and constant while it is not moving. The area of the orifice during the period where the valve is turned on and then off can be then modeled as:

$$A(t)=\begin{cases} \dfrac{A_o}{\tau_{open}}t & t<\tau_{open} \\ A_o & \tau_{open}<t<VOT \\ A_o-\dfrac{A_o}{\tau_{close}}(t-VOT) & VOT<t<VOT+\tau_{close} \\ 0 & VOT+\tau_{close}<t \end{cases} \tag{1}$$

where τ_{open} and τ_{close} are the times it takes for the valve to open and close, 10ms and 30ms respectively, *VOT* (Valve Open Time) is the specified time the valve is commanded to be held open, and A_o is the diameter of the orifice fully open. Since the solenoid and electronic control does not depend on the physics of the system and is commanded by the user, this is the function that will relate the orifice area to a given time t.

The mass flow of air through this orifice can be modeled using the *thin plate flow function* [6]:

$$\dot{m} = A(t)\cdot\phi(p_u,p_d) \tag{2a}$$

$$\phi(p_u,p_d)=\begin{cases} z(p_u,p_d) & \text{if } p_u \geq p_d \\ -z(p_d,p_u) & \text{if } p_u < p_d \end{cases} \tag{2b}$$

$$z(p_u, p_d) = \begin{cases} \alpha p_u \sqrt{\left(\frac{p_u}{p_d}\right)^{\frac{2}{\kappa}} - \left(\frac{p_u}{p_d}\right)^{\frac{\kappa+1}{\kappa}}} & \text{for } p_u/p_d \le \theta \\ \beta p_u & \text{for } p_u/p_d > \theta \end{cases} \quad (2c)$$

where the constants α, β and κ are defined in the appendix A. While the valve is closed, the system pressure is assumed to be equal to the pressure given by the lab pressure supply, while the pressure outside is assumed to be P_{amb} = 100,000 Pa.

Consider the case where the valve is actuated in the forward direction, with the lab pressure supply opening into the back chamber and the front chamber is exposed to ambient. Given $A(t)$, it is possible to calculate the mass flow rate $\dot{m}$ from the front chamber using the thin plate flow function.

In a MATLAB simulation [see Appendix B], this mass flow rate can be used with a sufficiently small time step Δt to predict the mass loss Δm from the front chamber at time t. From there, the ideal gas law is used, assuming the medium to be at room temperature and the system to be adiabatic during the process.

$$\Delta m = \dot{m} \Delta t \quad (3a)$$

$$P_F = \frac{(m_o + \Delta m)}{M} \frac{RT}{V_F} \quad (3b)$$

where m_o is the original mass of gas in the chamber, R is the ideal gas constant, T is the temperature of the gas, and V_F is the volume of the front chamber at time t. This outputs the change in pressure of the front chamber, which acts on the front of the piston of area A_{piston} with a force

$$F_F = A_{piston} P_F \quad (4)$$

The back chamber is directly open to the pressure supply, is assumed to be constant during this process, at P_{supply}. Thus, there exists a net force on the piston as the front pressure changes while the back does not. This net force F_{net} can then be used with kinematic equations governing the system, assuming no outside forces, to determine the acceleration a.

$$F_{net} = F_B - F_F \quad (5a)$$

$$a = \frac{(F_{net} - \eta v)}{m_p} \quad (5b)$$

With $a, x(t)$ can be calculated through a double integration over time. The unknowns in this model are the viscous losses coefficient η, the orifice diameter A_o, and the mass on the piston m_p. The orifice diameter can be measured from the area of the orifice at full opening, while the mass can be measured with a scale. The viscous loss can be determined through a simple test with the chambers both exposed to ambient (no net forces or pressure differences due to movement), while

a load is applied to the piston. By varying the loads and measuring the velocity of the piston, the coefficient of drag force to velocity can be experimentally determined.

This model now outputs the position profile $x(t)$ during the opening of the valve. Given a controlled input VOT, the ultimate displacement achieved can be predicted. As seen in fig. 5, this is modeled to be a linear relation. By scaling VOT, the final x position can be controlled. This will be the model behind the position control scheme.

4.2 Compliance Modeling

The model in the previous section predicts behavior of the system without any external loads besides the inertial load on the piston. In order to develop a force sensitive system, the force dynamics need to be studied. Due to the limited design, there is no method of actively changing the pressures inside the chambers besides the use of the on-off solenoid valve. From the previous section, the difference in pressures during actuation have been characterized to result in a F_{net} profile acting on the piston at no load. To determine the effects of a external force on the force and position profile, simply add the external load term to eq. 5a and compute from there.

When the system is at equilibrium, the force exerted by the piston will nominally be zero, as the pressures in the two chambers are equalized. If the system is then acted upon by an external force, without any valves opening, the natural compliance of the fluid medium, air, will respond with a certain force to displacement profile. By using the geometry and relations of the ideal gas law, the system stiffness can be calculated. Taking advantage of this system behavior allows for a simple method of position based force control, utilizing the natural compliance of the actuator to predict the force behavior.

Consider the cylinder at rest, with the piston extended x_o from its fully retracted position. At rest, the pressures of the two chambers are equal, at P_{supply}. The volumes of the two chambers are

$$\begin{aligned} V_B &= A_{piston} x_o \\ V_F &= A_{piston}(L - x_o) \end{aligned} \tag{6}$$

where V_B and V_F are the volumes of the back and front chambers, respectively, A_{piston} is the area of the piston inside the chambers, and L is the full length of the cylinder. Suppose now that the piston is forced to a new position x_f and is now at equilibrium. This causes a change in pressure in both chambers. Assuming the valves to be closed and that this is an adiabatic process, no mass has changed in either chamber so the ideal gas law can simplify to this relation.

$$V_o P_o = V_f P_f \tag{7}$$

We then get the relation between the initial and final pressures of each chamber – note that the area of the piston cancels out. This then leads to the calculation of the net force acted by the piston on the external force.

$$P_f = P_o \frac{x_o}{x_f} \tag{8}$$

$$F_{net} = A_{piston} P_{supply} \left(\frac{x_o}{x_f} - \frac{L - x_o}{L - x_f}\right) \tag{9}$$

The system compliance is determined by the ratio between the displacement and the force required to achieve that displacement. By creating a simulation utilizing the above

equations, a force-displacement profile can be generated for different values x_o. See fig. 6 for a plot of this relation. Note that the compliance is relatively linear for small displacements, and stays linear for larger displacements for initial positions near the middle of the cylinder.

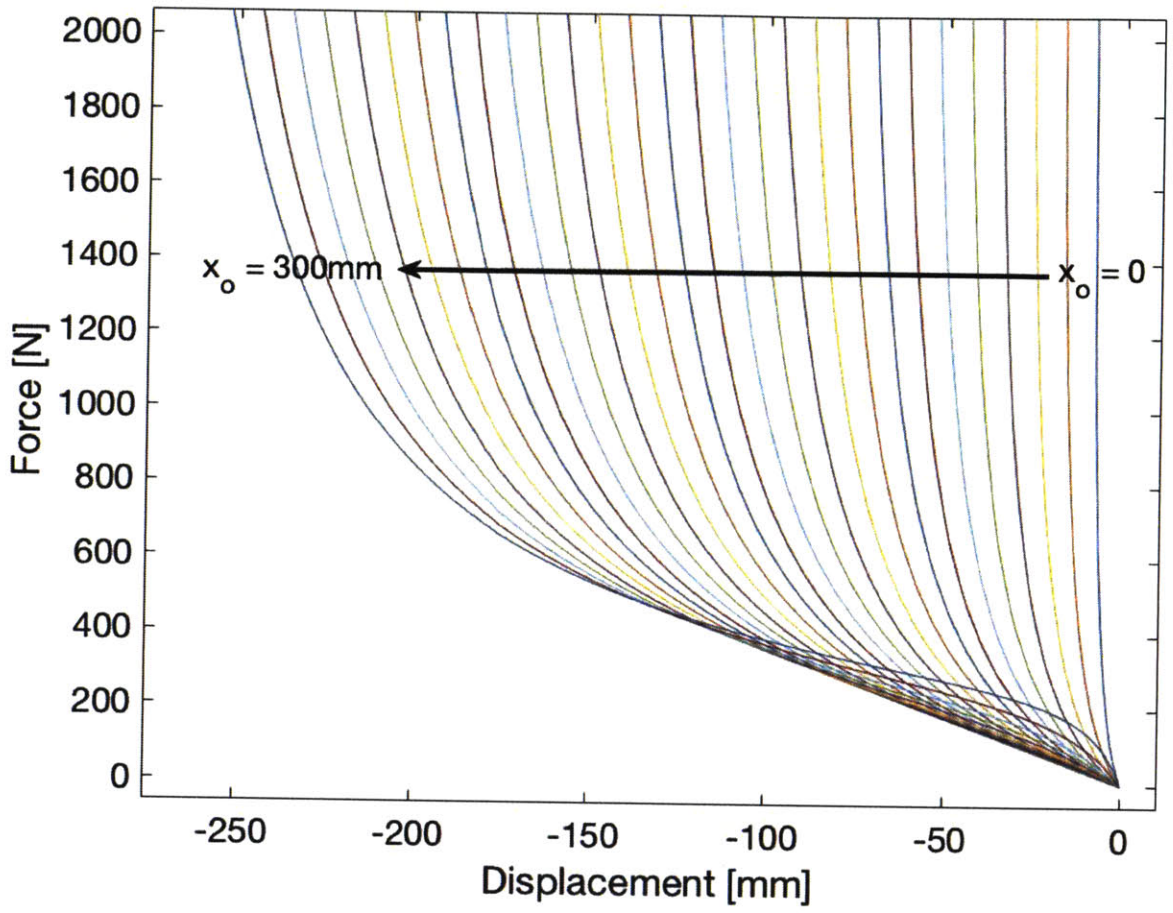

Fig. 6: Force - Displacement curves generated for different starting points xo of the system, from 0 to 300mm positions. Note the relative linearity of the curves for small displacements around starting points near the middle of the piston.

There exists now a method for theoretically determining the force output of the system forced from an extended position to a smaller position. This can be utilized with the position control scheme to create a force control scheme taking advantage of the system's natural stiffness. At any given position set point with a desired force output against a rigid structure such as the ground, the piston can be commanded to a calculable extra extension, that when the piston is then forced to the set point, it is exerting the desired force on the ground.

5 Characterization of Pneumatic System

5.1 Test Parameters and Process

To test the validity of the theoretical model of position behavior given valve acutation, the system was run at various *VOT* commands and pressures while measuring the displacement of the piston. This is an open loop configuration, where the position sensing is only used for data collection. Actuation signals were sent at the prescribed commanded time, while the system position response was collected. See fig. 9 for a schematic of this test. The system was given *VOT* commands at various starting positions X_o along the workspace of the actuator, and the position profile during each actuation recorded via sensing from the magnetopotentiometer. See table 1 for a full list of test configurations. Arduino code used for this test can be found in Appendix B.

Parameter	Range	Number of values
VOT	10-100ms	10
X_o	0-300mm	Varies per test config.
P_{supply}	0.33MPa - 0.69MPa	6

Table 1: Parameters of the tests for system characterization

The position data received can be seen in the example graph in fig. 7. After each actuation command signal was sent, a delay of 1s was introduced to ensure the system was at equilibrium before the next actuation, and to make post processing easier to determine where the initial and final position of each actuation was. Signal sent to the solenoid valve for actuation was also logged so that the experimental data could be lined up with the theoretical position profile.

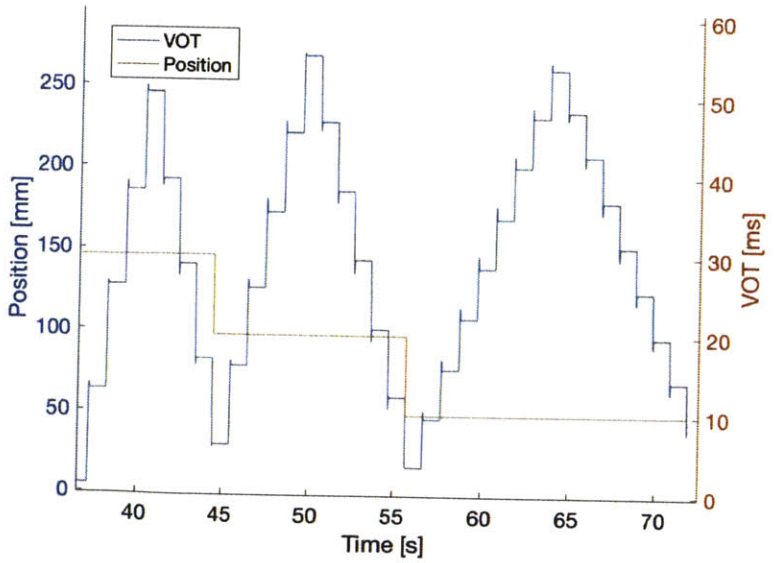

Fig. 7: Example data from characterization tests. Command signals with VOT windows were sent to the valve to push the leg to the edge of its workspace, then reverse to pull back and gather retracting data as well.

5.2 Data Processing and Model Comparison

After each test, the overall displacement from actuation Δx was plotted against to determine the function between the two. See fig. 10 for an overlay of the experimental position profile and the theoretical profile, along with displacements.

Once the data set is collected and processed, a linear fit function can be used to determine a function with input dx and output *VOT*, which is the model in the control scheme. This is of the form

$$VOT = A * \Delta x + B \tag{10}$$

where A and B are constants determined from the linear fit. For the 0.69MPa system, the constants were $\boldsymbol{A}$ **=18ms/mm** and $\boldsymbol{B}$ **=1.4ms** for the extending direction, and $\boldsymbol{A}$ **= -14ms/mm** and $\boldsymbol{B}$ **= -1.3ms** for the retracting direction. These constants were obtained from averaging data collected from 5 separate characterization tests of the same configuration.

5.3 Remarks and Observations

At lower pressures, it was seen that a linear fit was not enough to predict the behavior, and that the system had increasing position dependence on how far it would displace given a constant *VOT* command. See fig. 8 for detail. This is attributed to the increased compressibility of air at lower pressures, as well as a threshold force necessary to overcome the stiction force of the piston. However, at supply pressures above 0.5MPa, it was experimentally shown that the positional dependence became negligible, and that the limiting factor in actuation was the *VOT*.

As the system was designed for a supply pressure of 0.69MPa or higher, this model proved to be sufficient for supplementing the control behavior.

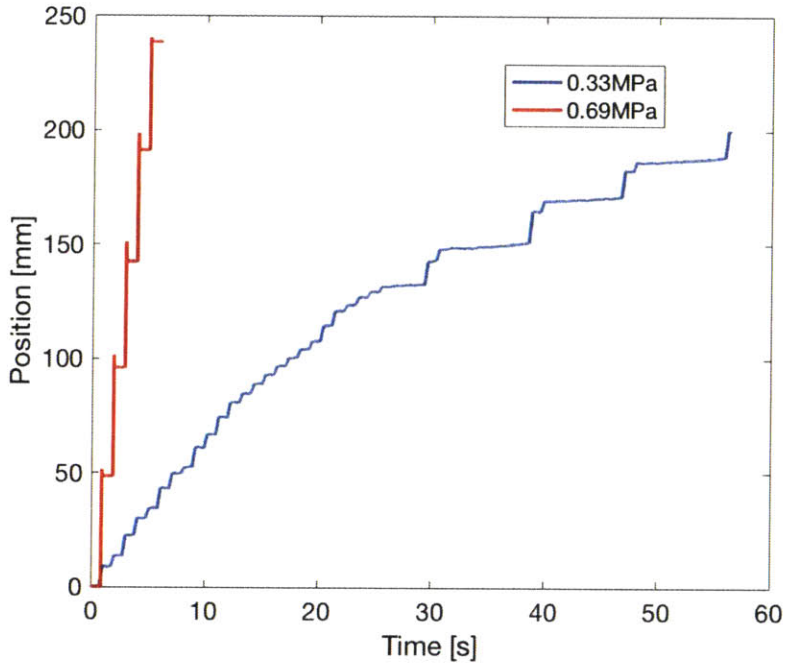

Fig. 8: Position tracking of piston being given constant VOT commands of 20ms. The low pressure system experiences more stiction the further out it is, reducing the displacement for each command time. The high pressure is consistent and linear through the entire span of the workspace.

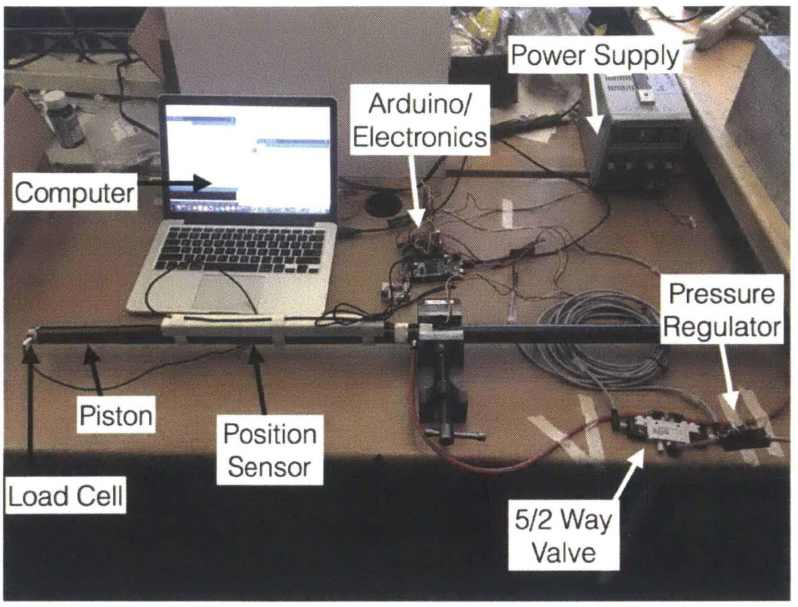

Fig.9: Schematic of bench top system for pneumatic characterization tests

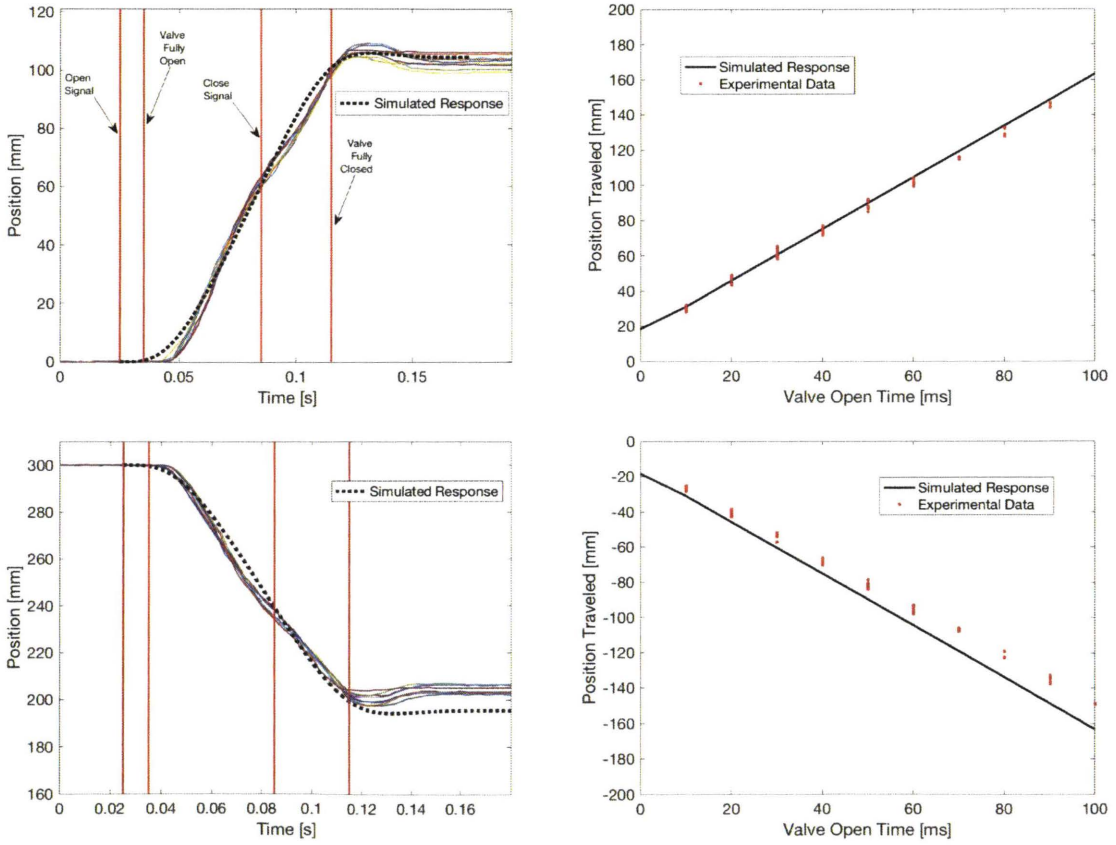

Fig. 10: (Top Left) Simulated response of a 60ms VOT at 0.69MPa in forward direction, overlaid over experimental data. Valve states at given times indicated by red vertical lines. (Bottom Left) Simulated response of same test in retracting direction, overlaid over experimental data. (Top Right) Overall displacement of actuator plotted against varying VOT in forward direction. Simulated response follows experimental data well. (Bottom Right) Overall displacement of actuator plotted against varying VOT in retracting direction. Note the experimental deviation from the simulation, possibly due to pressure losses in the longer tubing that feeds to the front chamber.

6 Position Control Scheme

With an accurate system model, an intelligent control scheme can be implemented. The system can be run with a simple open loop scheme using this model. Given a state of desired displacement and known supply pressure, a calculation utilizing the constants determined in the characterization shown in eq. (10) will output the necessary *VOT* for the piston to travel that distance.

6.1 Description of the Scheme

The proportional position closed loop control utilizes this model to output an actuation command, *VOT*, to the valve. Given a reference position, the error is calculated from the current position. This error is translated to a system *VOT* that will allow the piston to move that distance, theoretically reducing the error to 0. Once the command is given and the piston finished actuating, the position error is checked again and the loop re-run until the position is within a desired threshold. See fig. 11 for a diagram of the control scheme.

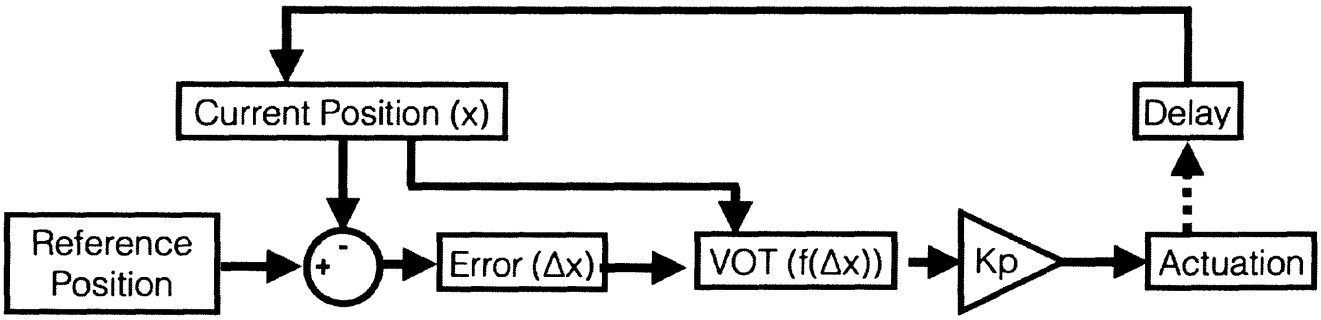

Fig. 11: Closed Loop Proportional Position Control Loop

6.2 Tuning Factors

Two factors are introduced to tune this scheme. The first is the delay and non-continuous behavior of the system, where no tracking or control occurs during the *VOT* command window. As a result, any perturbation of the system during this time will affect the actual displacement achieved, which will affect the overall time it takes for the system to reach the target position. This implies that having very fast cycles of *VOT* commands is useful to mitigate against this, where the system tries the open loop command as quickly as possible after the previous command was sent. However, due to the delay in closing time of the solenoid, it is not possible to have instantaneous tries, as this would cause the valve to be continually open, losing control on the system. Therefore, there is a "sweet spot" delay that needs to be implemented before each *VOT* signal that is not too small to not allow for the valve to close enough in a cycle, but not too slow to interfere with the speed requirements of the system. It was experimentally determined that a window of around 20ms provided reliable behavior.

The second factor is experimental inconsistency with the linear model and the actual condition of the actuator. Experimental characterization of the system showed slight deviation of the response of the actuator from the model, especially where factors such as pressure head and friction loss come into play. To bolster the system against these uncharacterized aberrations from the ideal case, a proportional gain constant was added to tune the *VOT* command signal. Keeping the

constant low (<1) allowed control of the overshoot of the signal, while high constants would create oscillatory, non-converging behavior. A gain of around 0.2 was used for the final prototype, with small variation between the left and right legs due to differences in the system during fabrication.

6.3 Control System Performance

With the two of these factors tuned correctly against each other, the control provided a relatively smooth and fast actuation of the leg for given reference positions. Step inputs spanning the length of the joint's workspace and a sinusoid wave were tested as position references while the system output position was tracked. See fig. 12 for plots of these tests. System characterization showed that the leg could fire from a fully closed position to the end of its workspace in ~200ms, with and overshoot of less than 0.5%.

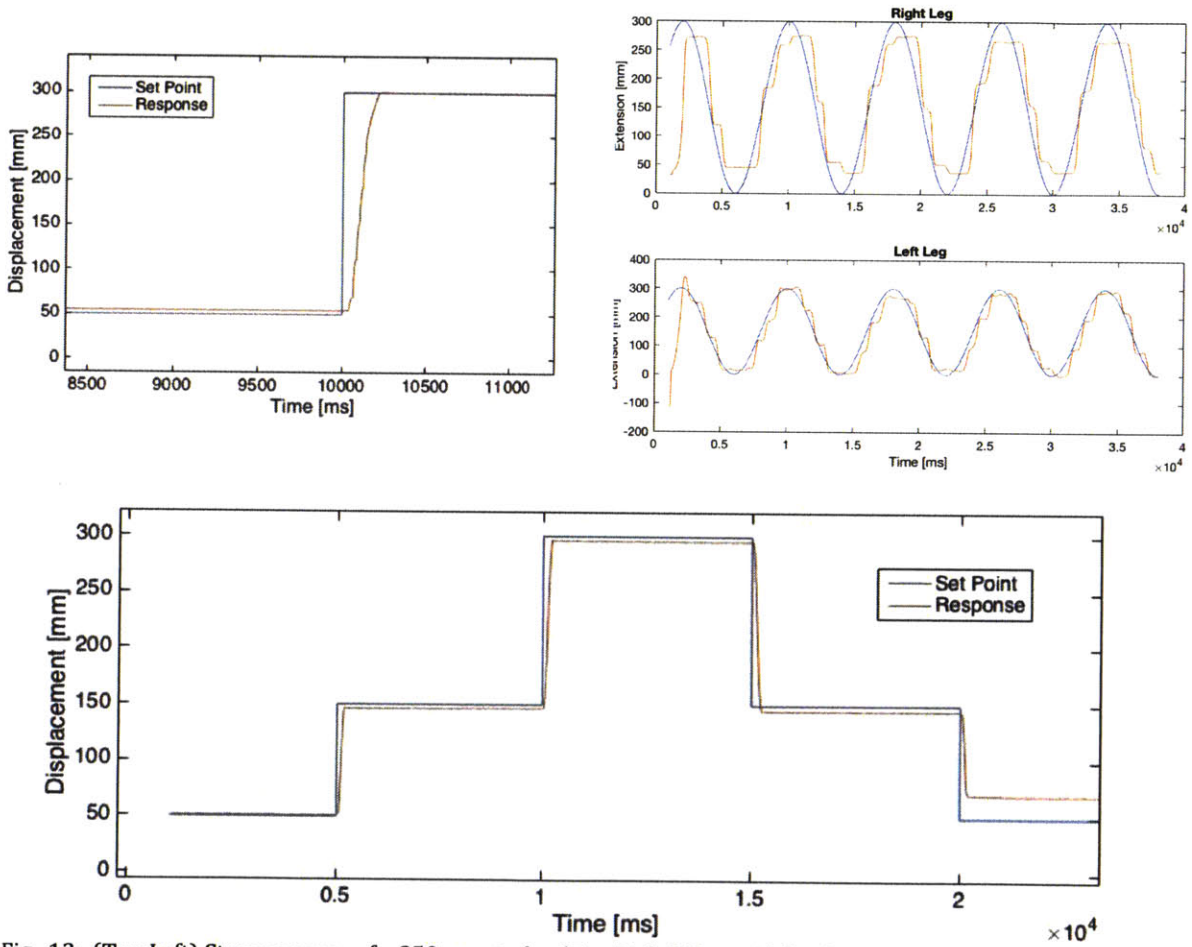

Fig. 12: (Top Left) Step response of a 250mm stroke. (Top Right) Sinusoidal reference tracking. (Bottom) Series of position commands, with tracking.

Smooth tracking of the sinusoid was more difficult to achieve, even with tuning the gain and delay. The control system relies on a set minimum magnitude of error before actuating, which provides the accuracy desired for this project (10mm) but prevents continuous tracking within these ranges. Similarly, the actuator has a minimum *VOT* command signal that will actually allow the piston to move. This was experimentally determined to be around 10ms, under which the system does not move. Due to the linear relation between the *VOT* signal and the error, as well as

the gain constant being less than 1, the system will be unable to fire for positional errors under a certain distance, which was experimentally observed to be between 10 and 50mm. This is analogous to a "stiction force" that many commercial actuators exhibit, namely a minimum actuation force that is required to make the system move. As seen in fig. 12 the system has rather discontinuous tracking of continuous smooth reference positions.

7 Load Control Scheme

Given the human interaction that this robot will encounter, safety in control and behavior will be necessary. Due to the high pressure of actuation and the inherent latency of pneumatic systems, this safety cannot be achieved with position control alone. It is useful to have a force sensitive implementation where the system compliance can be taken advantage of to maintain force control of the end effector. Certain tasks may require different compliances of the actuator, providing a desire to implement force control into this system.

7.1 Description of the Scheme

A basic force compliant scheme was implemented in this system where the stiffness of the actuation could be controlled using the load cell attached at the foot of the leg. Given a desired reference force that the actuator would need to be pressing, the force error could be calculated and multiplied by the theoretical actuator compliance ($1/K$) determined in section 4.2 to determine a new reference position. The position control scheme would then be implemented to push the actuator to the desired location. This will maintain the force using a basic error function, regardless of where the position of the actuator is. See fig. 13 for the scheme.

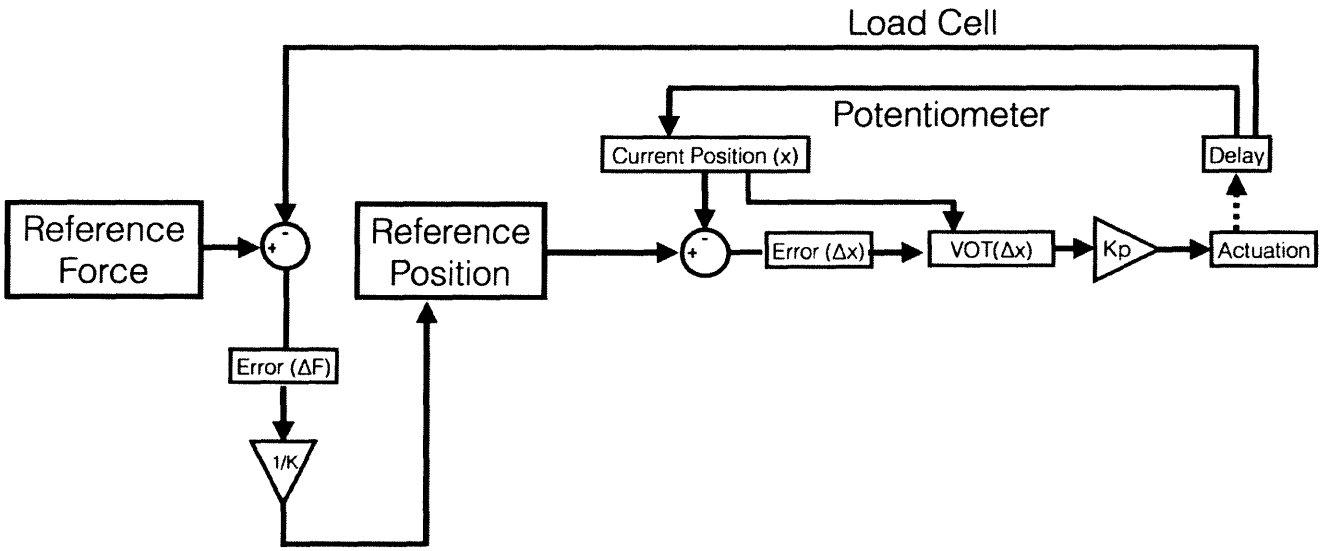

Fig. 13: Force Control scheme. The load reading is used to calculate the error from the reference, and multiplied with the system compliance to achieve a reference position.

7.2 Experimental Testing of Force Control

For a simple force control compliance test, the desired reference load was preset while the position of the actuator was externally perturbed. See fig. 14 for the setup. The desired load of the actuator was set at 25N, while the position of the endpoint was manually and randomly displaced with the rig. Position and force tracking of the actuator was collected and plotted in fig. 15. Note the relative smoothness of the position compliance, and the difficulty of the control scheme to maintain the set load. The load output is non-converging and erratic, with a variable range of about 50N, or 200%, implying a poor force control performance.

The set point load was increased to 100N and run on the bench top test. For the higher load, the variable range was around 100N, or 100%, which implied a better tracking ratio for higher loads. The setup was then taken off the bench top test and aligned vertically such that the load cell was contacting the ground directly. A force supplied by a human hand provided the position forcing input, while the control algorithm was run in this vertical configuration. The position forcing was run about 2X the speeds of the bench top test, yet the range of force tracking remained roughly within 100% of the desired load, implying little sensitivity to the speed at which the external loads are applied. It was noted that this configuration was similar to a cane, with variable stiffness, and was easily manipulated by the user.

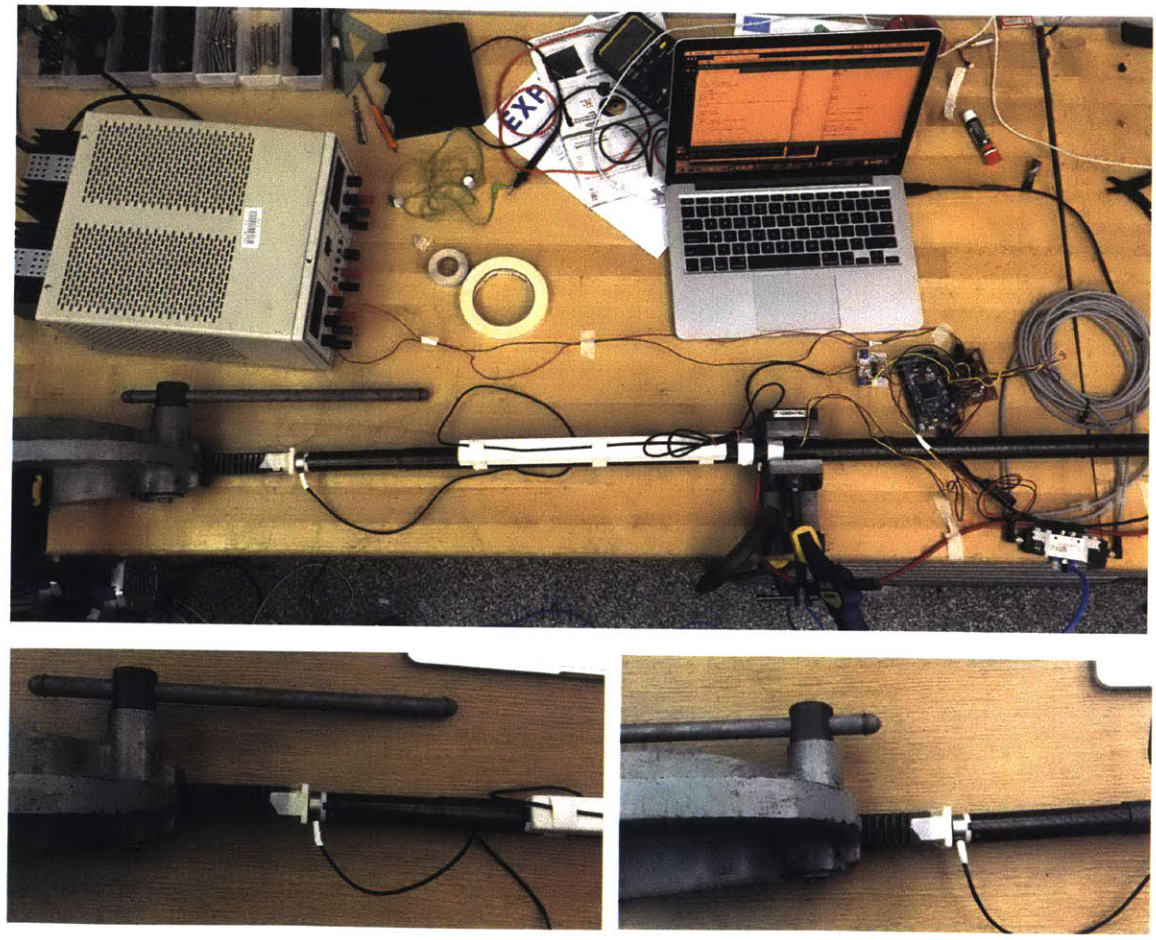

Fig. 14: (Top) Setup of the force control experiments. A heavy arbor press, seen on the left, was used to provide forced position inputs, acting on the tip of the leg where the force sensor is. This and the leg were clamped securely to the bench. (Bottom) Arbor press pushing forward and retracting on the end effector of the piston.

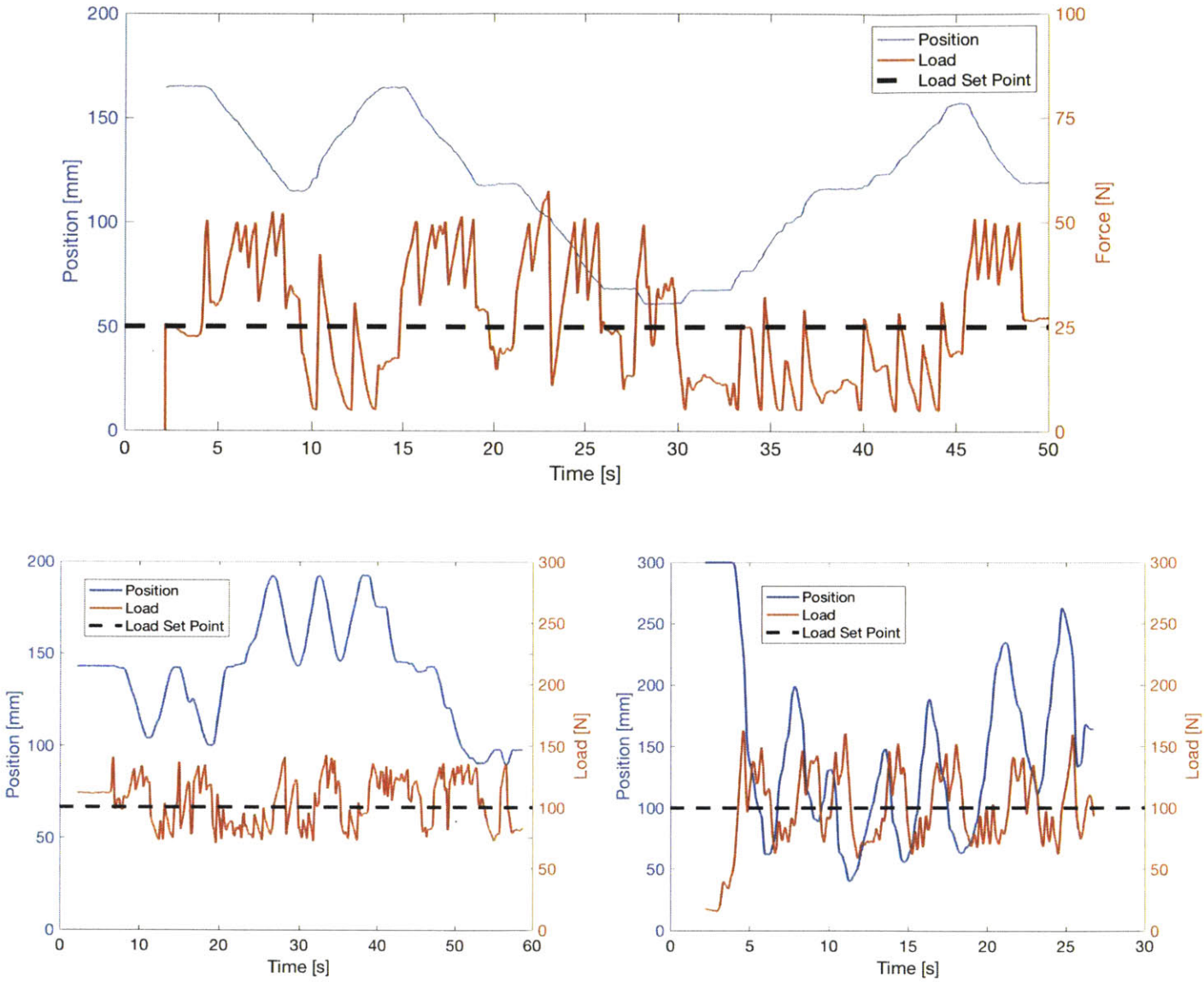

Fig. 15: (Top) Plot of position (blue) and load readings (red) for a benchtop test with a setpoint of 25N. Note the relatively smooth tracking of the position when perturbed to specific locations. The force tracking is much more erratic. (Bottom Left) Plot of benchtop test with a setpoint of 100N. (Bottom Right) Plot of upright test against ground, force provided by human hand, with a setpoint at 100N. Even with the fast variability of the human position forcing, the load stays within the same bounds as the slower benchtop test.

8 Application and User Testing

The actuator was twice fabricated, one for each leg, to be implemented in an assistive user test. With the robot strapped to the user in the harness, the ball joints were set at a fixed angle behind the user. The feet of the legs were set to the ground, and the actuator commanded to a preset cycle that would allow the user to move from a sitting to a standing position. See fig. 16 for images of the user wearing the robot.

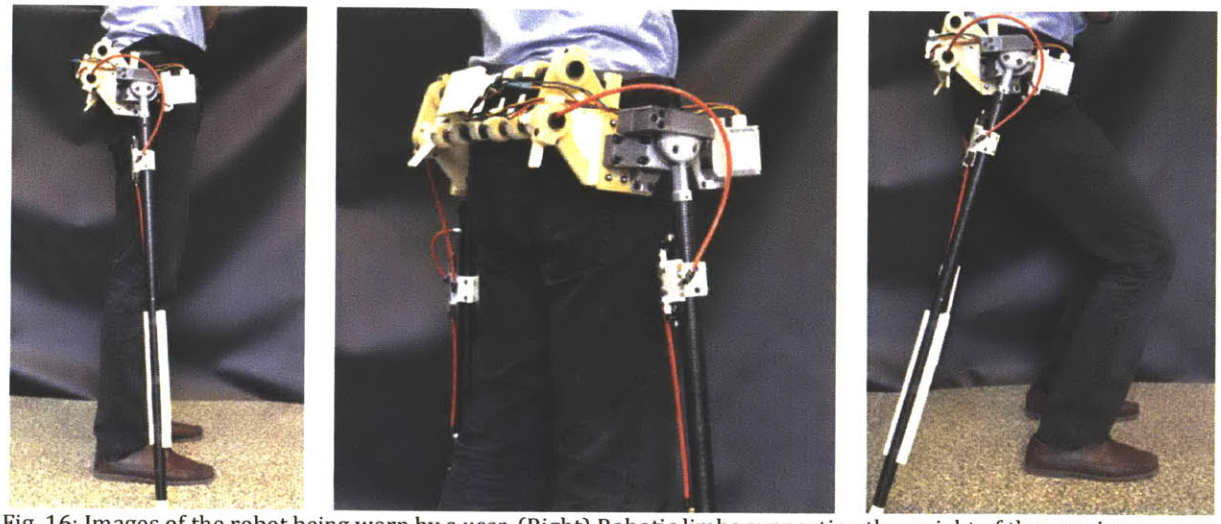

Fig. 16: Images of the robot being worn by a user. (Right) Robotic limbs supporting the weight of the user in a crouched position.

Position tracking during these tests was recorded to compare the user-loaded case with the benchtop response to step inputs. See fig. 17 for a comparison to the graph in fig. 12 in section 6. For these user tests, only the positional proportional control was implemented, as the load cells have not yet been integrated into the full system.

In these tests, the user attempted to put most of his weight on the robotic legs, utilizing his own legs as balancing points. The supply pressure was set at 0.69MPa, enough to lift most of the weight of the user. It is clear from the position tracking graphs that the added load (~60-90kg depending on the user) reduces the response time of the system, inducing large rise times (1-2 seconds), large overshoot, especially in the lowering direction and steady state error. However, due to the natural compliance of the pneumatics, the user is not ever subjected to hard, jerky motion. Even when the legs are retracting and overshoot too far, the motion is smooth, as if bouncing.

In total, two people have tested the current prototype of the SRL system and control. For both, the weight of the system was incredibly negligible. There were never any points in time when the user felt fatigued by the robot. The robustness of the leg design also held, with the user able to put his full sitting weight on the legs with complete support. Pads were utilized on the ground for the contact with the rubber feet due to the dustiness of the lab's floor area, but in normal conditions this is not necessary to provide enough traction. Comments include the system feeling like sitting on a chair, allowing the user to completely rest from leg support. Likewise, the user is projected to be able to stay in this crouched position much longer than if without the SRL system, which

provides a good use case for workers in the assembly field who may have to stay in awkward positions for long durations of time.

The power of the pneumatic actuator was readily showcased. At the 0.69MPa supply pressure, it was easily able to lift the user. This provides conclusive evidence that this actuation scheme will be strong enough to be beneficial for human use. Its assistive power in helping the user stand up from a sitting position allows it to become a natural aid for rehabilitation. The legs could even lift the user past the point where his foot contacted the ground, allowing for possible usages where the user may need to be more elevated than possible with human legs alone. See fig. 18 for a visual of this behavior.

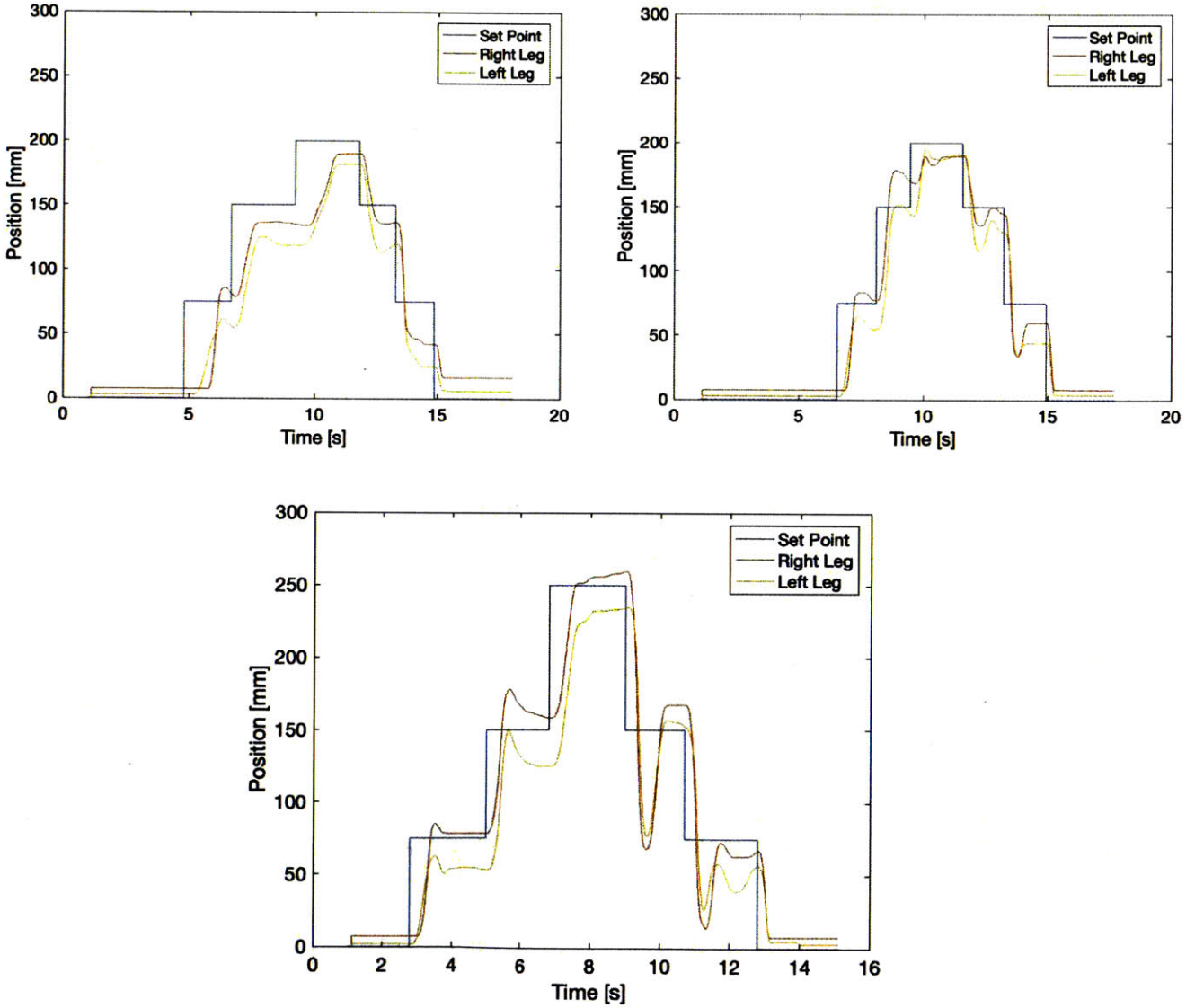

Fig. 17: Three separate user tests with positional control. (Top Left) Test showcasing large rise times and steady state offset. (Top Right) Data showcasing large overshoot. (Bottom) Higher displacements in the retracting direction show much higher overshoots than in the extending direction. In all cases, position tracking is fairly accurate to within the necessities of this project.

Fig.18: (Left) User in a sitting position, legs retracted. (Right) User in a hyperextended standing position, legs extended.

9 Conclusion

The SRL project has been an ongoing study on the integration of additional robotic limbs with human behavior. The possibilities for its assistive power in aiding human functionality are wide and promising. To that end, intelligent design of the systems that compose this wearable is essential for this research to become compelling and useful. The current prototype design of the SRL is the most compact, lightweight form yet; previous designs weighed tens of kilograms and were positioned awkwardly on the body. With the use of low weight high power servos, carbon fiber 3D printing, and simple pneumatic cylinder control systems, the SRL can be totally realizable as a non-inhibiting wearable device. Without the need for external exoskeletons or large actuation systems, the user is not encumbered by the design of the robot and can be solely supplemented by the robot, never hindered.

The design criteria have made for an interesting study on the pneumatic system, being limited from using more robust control systems with pressure regulation and sensing. In this system, the actuation is only controlled by a constant supply pressure and switching of an on-off solenoid valve. From theoretical modeling, the mechanical behavior of the pneumatic system can be predicted, discretizing the input as a desired displacement and the output a set opening time command. This function can then be validated with system characterization on bench top tests, and adjusted to fit the real system dynamics. Once a linear model relating the displacement and the valve opening time is obtained, an open loop control system can be utilized. By incorporating the position sensing from the linear potentiometer, the control loop can be closed and tuned with a proportional gain. Finally, the addition of a force sensor provides a closed loop method of controlling the force output of the pneumatic cylinder, which is supplanted with the theoretical model of the force versus displacement behavior of the system.

In a no-load scenario, the position control scheme has been shown to be extremely reliable, with steady state positional accuracy within 5mm, a rise time of 200ms for a 250mm stroke, and an overshoot of less than 1%. The loaded case, where a human is wearing the system, puts more of a strain on this control system. Depending on the weight of the user, position accuracy can be offset by 20mm, with rise times one the order of seconds and high overshoot. In order to improve the control of this system, the external load on the leg must be addressed and compensated for.

Force control of these actuators with the proposed scheme was shown to be less reliable, with oscillations of 50-100N for the set point loads tested. Prior research has shown force control to be achievable with pneumatics, but is made much easier with closed loop pressure control. It is inconclusive from this study's findings whether or not the on-off solenoid valve can be used to achieve reliable force control, or if the latency in dynamics of the pneumatic system will continually prevent oscillations from being tuned away.

Further study of the control systems can greatly increase the usability of these actuators in this system. It is suggested that a PID controller on the position feedback could allow for tuning that diminishes the non-desired latency and overshoot of the loaded scenario. Load control schemes that incorporate more complex controllers may also prove fruitful. A position-load hybrid scheme may even produce better results, where the physics of the position profile is used in conjunction with the load sensing output to better model behavior during use on a wearer.

The user application for the current system has shown to be very promising for the overall SRL project. The user is completely unencumbered by the weight of the robot, while the robustness

and power of the pneumatic scheme provides the exact benefit required. Further testing of the system with integration of all actuators will be able to showcase the benefits of the system as a whole. Use case studies including assistive rehabilitation for weak and elderly patients in standing and walking have been proposed. From initial user testing, it is clear that the legs have augmentative power as well, allowing the human body to be positioned in ways that could not be sustained normally. Further development of control profiles for these specific use cases will be necessary to showcase the robot's potential in these fields.

Appendix A – Specifications on Components of the Robot

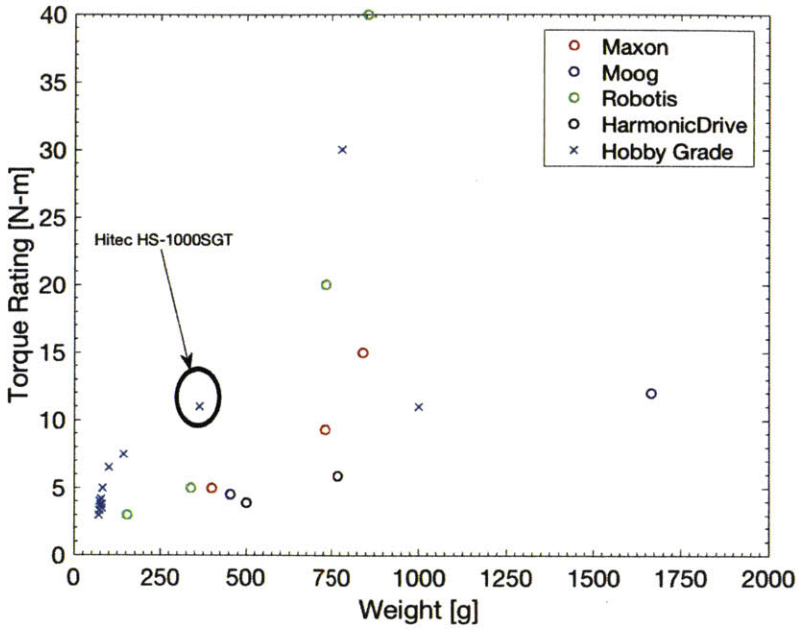

Plot of the various commercially available options of motors searchable online, in the weight and torque class desired. The circled point is the chosen motor, the Hitec HS-1000SGT, and outperforms the hobby most hobby grade motors with double the torque, whiles still being as light as the weaker industrial grade motors.

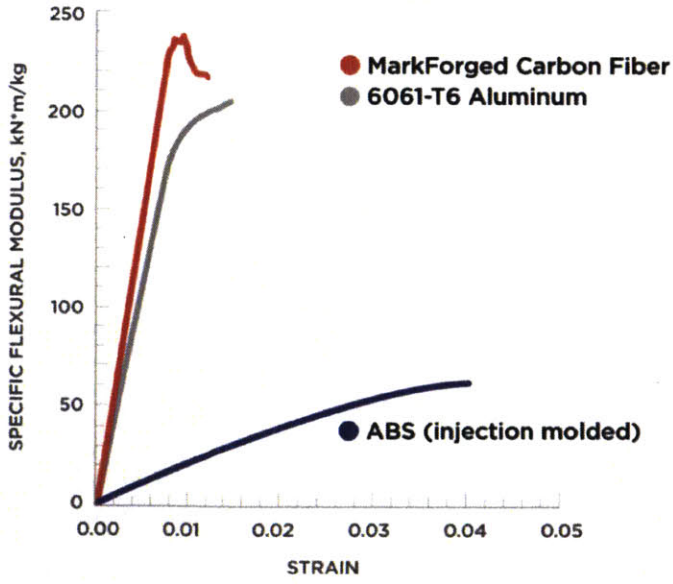

Stress-strain curve of the 3D printed carbon fiber parts by MarkForged. They show comparable stiffness to aluminum.

Double Acting – **0875D04-00A**
Double Nose or Rear Pivot Mount

Standard Stroke Lengths: 1/2", 1", 1-1/2" 2", 2-1/2", 3", 4", 5", 6"

Maximum Stroke: 32"

Base Weight: .32 lbs., plus .03 lbs. per inch of stroke

*Optional Accessories:
- M117005 Mounting Bracket
- M129003 Pivot Bracket
- M127003 Rod Clevis

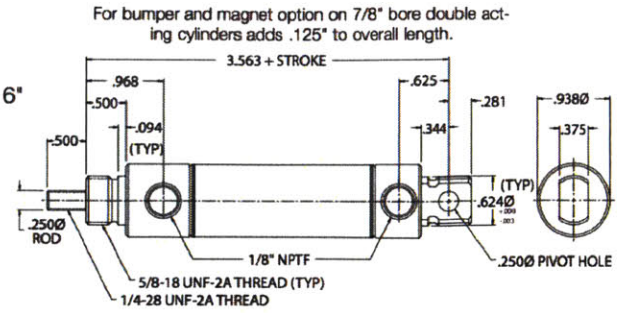

Specifications on the pneumatic cylinder used to actuate the leg, from Numatics.

Solenoid valves VUVG-L10 and VUVG-S10, in-line valves M5

FESTO

Technical data

General technical data														
Valve function			T32-A			T32-M			M52-R	B52	M52-M	P53		
Normal position			C[1]	U[2]	H[4]	C[1]	U[2]	H[4]	–	–	–	C[1]	U[2]	E[3]
Stable position			Single solenoid							Double solenoid	Single solenoid	Single solenoid		
Reset method: pneumatic spring			Yes			No			Yes[5]	–	No	No		
Reset method: mechanical spring			No			Yes			Yes[5]	–	Yes	Yes		
Nominal size		[mm]	2.7			1.9	1.8		3.2		2.2	3.2		
Nominal flow rate		[l/min]	150			135	125	125	220		190	210		
Flow rate on manifold rail		[l/min]	150			135	125	125	220		190	210		
Switching time on/off		[ms]	6/16			8/11			7/19	–	8/24	10/30		
Changeover time		[ms]	–							7	–	16		
Width		[mm]	10											
Port	1, 2, 3, 4, 5		M5											
	12/14		M3											
Product weight		[g]	55			54			45	55	44	55		

Operating and environmental conditions								
Valve function			T32-A[1]	T32-M[3]	M52-R[2]	B52	M52-M[3]	P53
Operating medium			Compressed air in accordance with ISO 8573-2010 [7:4:4]					
Operating pressure	Internal	[bar]	1.5 ... 8	2.5 ... 8	2.5 ... 8	1.5 ... 8	3 ... 8	3 ... 8
	External	[bar]	1.5 ... 10	–0.9 ... 10			–0.9 ...8	–0.9 ... 10
Pilot pressure[4]		[bar]	1.5 ... 8	2 ... 8	2.5 ... 8	1.5 ... 8	3 ... 8	
Ambient temperature		[°C]	–5 ... +50, –5 ... +60 with holding current reduction					
Temperature of medium		[°C]	–5 ... +50, –5 ... +60 with holding current reduction					

Specifications on the solenoid valve used to route pressure into the chambers of the pneumatic cylinder, from Festo.

Appendix B – MATLAB and Arduino Code used in the system

MATLAB simulation of the pneumatic system given various *VOT* actuation commands.

```
clear all

P = 689476;%Pa
forward  = 1;
VOT = (10:10:100)*1e-3;%s
lvot = length(VOT);
x0=0; %m
x(1:lvot,1) = x0*1e-3; %m

R = 8.31; %Pa*m^3/mol/K
T = 293; %K
Psupply = P;
Patm = 100000; %Pa
t = (0:.1:300)*1e-3; %s
dt = t(2)-t(1);
orifice_D = 1.85e-3; %m
A0 = 3.14*(orifice_D)^2/4; %m^2
k = A0/10e-3; %m^2/s
M = .029; %kg/mol
Apb = 3.14*.022225^2/4; %m^2;
Apf = Apb;% - 3.14*.00635^2/4; %m^2
L = 300e-3; %m
D = .022225; %m
mp = 100e-3; %kg

Pf(1:lvot,1) = Psupply;
Pb(1:lvot,1) = Psupply;

Vf(:,1) = (L-x(:,1))*Apb-(L-x(:,1))*(Apb-Apf);
Vb(:,1) = x(:,1)*Apb;

mf(:,1) = Pf(:,1).*Vf(:,1)*M/R/T; %kg
mb(:,1) = Pb(:,1).*Vb(:,1)*M/R/T; %kg
Ff(:,1) = Pf(:,1)*Apf;
Fb(:,1) = Pb(:,1)*Apb;
Fnet(:,1) = Fb(:,1)-Ff(:,1);
a(1:lvot,1) = 0;
v(1:lvot,1) = 0;

for j = 1:length(VOT)
for i = 1:length(t)-1

    if t(i)<=10e-3
        A(j,i) = k*t(i);
    elseif t(i)<=VOT(j)
        A(j,i) = A0;
    elseif t(i)<=VOT(j)+30e-3;
        A(j,i) = A0-k/3*(t(i)-VOT(j));
    else
        A(j,i) = 0;
    end

        mfdot(j,i) = A(j,i)*phi(Pf(j,i),Patm);
        dmf(j,i) = -mfdot(j,i)*dt;
    if forward

        mf(j,i+1) = mf(j,i) + dmf(j,i);
        Pf(j,i+1) = mf(j,i+1)/M*R*T/Vf(j,i);
        Ff(j,i+1) = Pf(j,i+1)*Apf;

         Pb(j,i+1) = Pb(j,i);
         Fb(j,i+1) = Pb(j,i)*Apb;
    else
        mb(j,i+1) = mb(j,i) + dmf(j,i);
        Pb(j,i+1) = mb(j,i+1)/M*R*T/Vb(j,i);
        Fb(j,i+1) = Pb(j,i+1)*Apb;
```

```
            Pf(j,i+1) = Pf(j,i);
            Ff(j,i+1) = Pf(j,i)*Apf;
        end
        Fnet(j,i+1) = Fb(j,i+1)-Ff(j,i+1);
        a(j,i+1) = (Fnet(j,i+1)-(v(j,i))*15)/mp; %viscous damping
        v(j,i+1) = v(j,i) + a(j,i+1)*dt;
        x(j,i+1) = x(j,i) + v(j,i+1)*dt;
        Vf(j,i+1) = (L-x(j,i+1))*Apb-(L-x(j,i+1))*(Apb-Apf);
        Vb(j,i+1) = x(j,i+1)*Apb;
    end
    end
```

Arduino code for open loop air cylinder characterization tests.

```
float openTime = 100;
float i = 0;
int SIG = 0;
int DIR = 0; //0 is FORWARD, 1 is BACKWARD;
float POT;
int flag = 0;
float PRESSURE;
float timenow;
int n = 1;
float tic;
float toc;
int valve1 = 5;
int valve2 = 4;
float high = 800;
float low = 150;

void setup() {
  // put your setup code here, to run once:
Serial.begin(115200);
pinMode(valve1,OUTPUT);
pinMode(valve2,OUTPUT);
digitalWrite(valve1,LOW);
digitalWrite(valve2,LOW);
i = millis();
}

void loop() {
  // put your main code here, to run repeatedly:
  PRESSURE = analogRead(0);
  POT = analogRead(1);
   timenow = millis()-i;
   if(openTime>0){
     if(timenow < openTime){
       SIG = 1;}
     else if(timenow < openTime+1000){
       SIG = 0;}
     else{ i = millis(); SIG = 0;}

     if(POT<high & POT>low & DIR==0)
       {}//digitalWrite(valve2,SIG*255);digitalWrite(valve1,LOW);}
     else if(POT>high & DIR==0)
       {DIR = 1;}
     else if(POT>low & POT<high & DIR==1)
       {}//digitalWrite(valve1,SIG*255);digitalWrite(valve2,LOW);}
     else if(POT<low & DIR==1)
       {DIR = 0; flag = 1;}

     if(DIR==0){digitalWrite(valve2,SIG*255);digitalWrite(valve1,LOW);
     else{digitalWrite(valve1,SIG*255);digitalWrite(valve2,LOW);}


    Serial.print(millis()); Serial.print(',');
    Serial.print(POT); Serial.print(',');
    Serial.print(SIG); Serial.print(',');
    Serial.print(DIR); Serial.print(',');
    Serial.print(openTime);  Serial.print(',');
    Serial.print(PRESSURE); Serial.println(';');

    if(flag == 1){
       openTime = openTime-10; flag = 0;

       }
    }
  }
```

Bibliography

[1] F. Parietti and H. Asada, "Supernumerary Robotic Limbs for Human Body Support," *IEEE Trans. Robot.*, vol. 32, no. 2, pp. 301–311, Apr. 2016.

[2] J. A. Linnett and M. C. Smith, "An Accurate Low-Friction Pneumatic Position Control System," *Proc. Inst. Mech. Eng. Part B J. Eng. Manuf.*, vol. 203, no. 3, pp. 159–165, 1989.

[3] R. B. van Varseveld and G. M. Bone, "Accurate position control of a pneumatic actuator using on/off solenoid valves," *IEEEASME Trans. Mechatron.*, vol. 2, no. 3, pp. 195–204, Sep. 1997.

[4] K. Ahn and S. Yokota, "Intelligent switching control of pneumatic actuator using on/off solenoid valves," *Mechatronics*, vol. 15, no. 6, pp. 683–702, Jul. 2005.

[5] M. Taghizadeh, A. Ghaffari, and F. Najafi, "Modeling and identification of a solenoid valve for PWM control applications," *Comptes Rendus Mécanique*, vol. 337, no. 3, pp. 131–140, Mar. 2009.

[6] Y. Tassa, T. Wu, J. Movellan, and E. Todorov, "Modeling and Identification of Pneumatic Actuators," 2013.